Mattila, T.; Nieminen, R.M.; Dzugatoo, M.

Simulation of radiation-induced structural transformation in amorphous metals

Simulation of radiation-induced structural transformation in amorphous metals

T. Mattila* and R. M. Nieminen[†]

Laboratory of Physics, Helsinki University of Technology, 02150 Espoo, Finland

M. Dzugutov[‡]

Center for Parallel Computers, Royal Institute of Technology, 100 44 Stockholm, Sweden

(Received 19 May 1995)

Molecular-dynamics simulations investigating the radiation-induced structural transformations in metallic glasses are reported. We have studied three models of an equilibrium simple glass, possessing a pronounced icosahedral local order. Two of these are monatomic and one represents the amorphous Ni-P alloy. A detailed analysis of the evolution of the structural damage induced by irradiation is presented. In all the systems, a persistent residual reduction in icosahedral order is observed. An important finding of this study is that the metallic glasses are able to sustain a considerable increase in the number of vacancies which arises as a result of the irradiation-induced structural transformation.

I. INTRODUCTION

Some metallic systems under rapid cooling are able to form glasses, metastable solid phases with liquidlike structure. Glassy metals demonstrate a range of unique and technologically interesting properties as compared to their crystalline counterparts. Among the most important of these is the singular ability of metallic glasses to sustain the local structural damage induced by irradiation. Although the connection between this phenomenon and the noncrystalline structure of glasses is apparent, very little is known about the actual behavior of the structure when a collision cascade caused by the collision between a constituent atom and a high-energy particle induces a local structural perturbation. Because of inherent limitations of the existing experimental methods of structural analysis, the molecular-dynamics simulation technique (MD) remains a unique and powerful tool for investigating the microscopic transformations in the glassy structures caused by irradiation.

There is a large volume of evidence supporting the idea, suggested by Frank,[1] that the ability of glass-forming metallic alloys for strong undercooling is crucially related to the icosahedral short-range order (ISRO) which has been established as a distinctive structural feature of these systems. The prominent role of icosahedral ordering in formation of metallic structures has been realized in the last decade following the remarkable discovery by Schechtman *et al.*[2] of a solid metallic phase with global icosahedral symmetry. Icosahedral arrangement in the nearest-neighbor shell is a closest approximation to tetrahedral packing which is assumed to be favored by energy. However, in contrast to other local densely packed units, icosahedra cannot fill the space without frustration. Therefore, besides the fivefold configurations characteristic of ISRO, the structure has to include nonicosahedral structural units: bonds with fourfold and sixfold coordination symmetry. Landau theory[3] indicates that the process of structural relaxation in a system with ISRO leads to the formation of disclination lines comprised of these bonds. As the system relaxes to the ground state, only the sixfold ones are expected to survive as more energetically favorable,

forming a pattern with a long-range order. In most of the cases, this is a Frank-Kasper periodic structure, but the relaxation of ISRO can also lead to the formation of a quasicrystalline structure. The described process of ordering of disclination lines into a regular structure is a highly cooperative phenomenon which requires a concerted rearrangement of large groups of atoms. Therefore, it can be blocked by a rapid enough cooling, whereby the disclination lines become entangled in a disordered network, corresponding to a glassy structure.

The rich variety of stable and metastable phases in metallic systems, associated with ISRO, thus arises from the competition between the local icosahedral ordering and the long-range frustration. Therefore, mutual transformations of these phases as well as their stability with respect to external perturbations, such as radiation-induced damage, depends crucially on the statistical balance between the icosahedral and the nonicosahedral local structural units. Recently, it has been found that the presence of icosahedral quasicrystalline inclusions stabilizes the structure of steel by impeding the spreading of dislocations.[4] In multicomponent metallic glasses, the mechanisms of local structural relaxation involves transformation of the chemical ordering, and it is of profound importance to discern this aspect of structural evolution from the transformation of the topological order. An important advantage of the MD method is that it allows to investigate separately the latter process by simulating the glassy state in a monatomic model.

Laakkonen and Nieminen[5] have used MD simulation to investigate the irradiation effects in a quenched Lennard-Jones (LJ) system. They found that the interstitials and vacancies created by the collision cascade disappear rapidly at the early stages of the following structural relaxation, and no appreciable net creation of these defects was observed. In this study, we employ the MD simulation to investigate the radiation-induced structural transformations in more realistic models which represent metallic glasses possessing pronounced local icosahedral order. We demonstrate that these models, in contrast to the LJ system, are able to sustain a considerable rate of thus induced permanent structural dam-

53   192

age. A most interesting feature observed is a net increase in the number of vacancies.

The paper is organized as follows. In Sec. II we describe the MD method and the three models used for glassy metals. In Sec. III the glassy state preparation procedure is outlined, the structure analysis of the glassy state with ISRO is described in detail and results regarding the structure of the obtained glassy systems are presented. Section IV continues with the procedure for radiation damage simulations and the results of these simulations are collected and discussed in Sec. V. Finally in Sec. VI the conclusions are drawn.

II. SIMULATION METHOD

A. Molecular dynamics

All the glassy systems studied were prepared by cooling from melt. This could easily be accomplished in MD simulation by first equilibrating the system well above the melting temperature and then rapidly reducing its kinetic energy. After relaxing the quenched system to a metastable equilibrium state, the radiation damage simulations could be carried out. The interaction between radiation and the glassy material was simulated by assigning a momentum to a chosen atom which imitated its collision with a high-energy particle, e.g., a neutron. A thorough structural analysis was performed to describe the changes in the ISRO during the recoil initiated collision cascade. A detailed description of this analysis will be given below.

The simulations were carried out using systems consisting of 16 384 atoms. The large system size is an essential prerequisite for creation of a realistic model of the glassy phase.[6,7] It improves statistical accuracy of the monitored structural characteristics describing the amorphous system. Furthermore, in the radiation damage simulations, the large system size allows the use of high recoil energies of up to several keV. The inevitable disadvantage of using a large system is the heavy computational cost. In this study the MD program was optimized by using linked neighbor lists and tabulated forces. Due to these techniques the computational time depended linearly on the number of atoms and the calculations could be carried out using conventional RISC workstations. The simulations were based on the velocity version of Verlet algorithm and to control the temperature we used the standard Nosé method.[8]

B. Pair potential model

Simple metallic glasses are known to be formed by multicomponent metallic alloys, whereby the effects of chemical ordering play a very significant role. A recent study, however, demonstrated that a large degree of ISRO can be induced in a simple monatomic liquid by using a specially constructed form of pair potential.[6,7] The structure of this liquid, imitating that of metallic glass-forming alloys, also shows good agreement with the conjectures of the Landau theory of icosahedral ordering.[3] A remarkable distinction of the liquid is its pronounced glass-forming ability. While remaining in an equilibrium liquid domain above the melting point, it can be cooled to a singularly viscous state, demonstrating pronounced non-Arrhenius behavior characteristic of the liquid-glass transition region.[9]

A usual crystallization pattern for the metallic glass-forming alloys is a Frank-Kasper structure. However, the described monatomic glass-forming model, having been slowly cooled below the melting point, forms a dodecagonal quasicrystal.[10] The stability of quasicrystal-forming alloys under supercooling has been observed recently,[11] and it was found that the phase transition in those systems shows a number of interesting thermodynamical distinctions as compared with crystallization in conventional glass formers.

An important structural feature of this model is the presence of intermediate-range order, indicated by an anomalous long-wavelength prepeak in the structure factor. It can be attributed to the formation of a network which is presumably related to the growth of disclination lines. It has to be mentioned that the anomalously high viscosity of this liquid observed at the melting point was found to be associated with the change of the diffusion mechanism. Close to the melting point, the latter demonstrated a contribution due to activated hopping, which indicates the presence of vacancies.[9] Thus, the system appears to be able to sustain a considerable density of vacancies already in the liquid domain. This observation seems to be consistent with a conjecture that the long-wavelength prepeak in the structure factor of glassy systems can be attributed to the locally ordered network of vacancies.[12]

Due to the high viscosity of the model liquid at the melting point, the described quasicrystallization can easily be avoided by applying a sufficiently rapid cooling. The system then forms a solid amorphous phase, which can sustain its structural stability in a long simulation run. Thus, the system can be regarded as a generic glass former. It represents an attractive prototype monatomic model of metallic glass forming alloys which can be used to investigate radiation-induced structural transformations in these materials. Hereafter this model will be referred to as model I.

C. Embedded atom models

In the known Ni-P glassy metals the phosphorus content varies usually from 20 to 30%.[13] This metal-metalloid compound was chosen to be studied because of the major Ni part which can be reliably modeled with the embedded-atom method (EAM).[14] For modeling metallic glassy systems EAM provides a computationally efficient tool which rivals well the more complex tight-binding based models.[15,16] In this study two EAM-based models were used: a monatomic model of pure supercooled Ni (referred to as model II) and an otherwise similar second model except for a 25% phosphorus fraction (referred to as model III). The monatomic model II was introduced in order to have a one-component reference system for model III with the lighter P atoms.

The functional forms of the EAM functions in this study were closely related to the ones used by Johnson.[18] The EAM parameters were fitted[17] by calculating the total energy of an fcc lattice as a function of lattice constant and comparing the obtained curve to the one given by Rose et al.[19] The values used in constructing the reference curves are given in Table I. For Ni the values are based on the experimental values.[20,21] However, for the $Ni_{75}P_{25}$ compound we were not aware of proper experimental data. Therefore a series of self-consistent density-functional calculations were performed.[22] The method used linear muffin-tin orbitals, atomic-sphere

TABLE I. The values of parameters used in creating the reference curves for fitting the EAM parameters.

Material	a_0(Å)	B (10^{11} Pa)	E_c (eV)
Ni	3.52	1.82	-4.45
P	3.80	0.77	-3.4
$Ni_{75}P_{25}$	3.50	1.87	-4.3

TABLE II. The parameters for the high-energy corrections in the EAM models.

Atom pair	r^*(Å)	ϵ (eV)	κ
Ni-Ni	1.6	17.0	5.5
P-P	1.6	12.0	5.5
Ni-P	1.6	12.0	5.6

approximation and the local-density approximation (LDA). The total-energy curves as a function of lattice constant were calculated for Ni, P, and $Ni_{75}P_{25}$. The chosen ratio for the Ni-P compound allowed the use of a single four atom unit cell with periodic boundary conditions. Based on the data from LDA calculations the reference values for P and $Ni_{75}P_{25}$ were introduced.

In order to avoid discontinuities in the EAM functions the cutoff was performed smoothly with the help of trigonometric functions. In both EAM models the smoothing was performed between 3.0 and 3.8 Å, so that when the interparticle separation exceeded the latter criterion all interactions were neglected. Because the fcc lattice constant for Ni is 3.52 Å, the chosen values for the cutoff region lead also to second nearest-neighbor interactions. This is essential for the present application because the region between first- and second-nearest-neighbor shells is essential for the formation of ISRO.

The original EAM scheme cannot directly be applied to simulations where high-energy collisions with energy transfer up to several keV may occur. The energy region where the original EAM is valid is limited to a few tens of electron volts and the model must therefore be modified to be applicable for the present purpose. At short distances between the atoms the many-atom interactions can be safely neglected and the total interaction can be described by a pair potential. Realistic high-energy pair potentials can be obtained using the density-functional approach with the commercial DMol program.[23] Using this method high-energy pair potentials for the Ni-Ni, P-P, and Ni-P dimers were calculated.[24] These high-energy potentials were combined to the EAM scheme by modifying the repulsive pair potential already present in EAM. However, the functional form of the original EAM pair potential cannot be fitted to be valid at both lattice equilibrium and small distances. To avoid discontinuities in the modified repulsive potential and its derivative, the following scheme was introduced:

$$\phi(r) = \phi_{\text{EAM}}(r) + \epsilon(r-r^*)^2 e^{-\kappa[(r/r^*)-1]}, \quad r<r^* \quad (1)$$

$$\phi(r) = \phi_{\text{EAM}}(r), \quad r \geq r^*, \quad (2)$$

where $\phi(r)$ and $\phi_{\text{EAM}}(r)$ denote the modified repulsive pair potential and the corresponding original one and r^*, ϵ, and κ are the parameters to be fitted.

In Eq. (1) the latter term on the right-hand side includes a parabola which has its minimum at r^*. Multiplied by the exponential term and added to the original EAM pair potential $\phi_{\text{EAM}}(r)$, the parameters ϵ, κ, and r^* can be chosen so that (1) approximates well the density-functional based potential when $r<r^*$. The parabola makes the pair potential as well as the derivative continuous. Thus it remains to find a

proper value for r^*, which represents the correction limit, and for the values of the other parameters stated above. These values are presented in Table II. The fit was made so that the modified EAM model described the interactions properly up to 5 keV. As an example, the energy of the Ni atom approaching another Ni atom is presented in Fig. 1. For comparison, the energies calculated by the original and modified EAM models are shown together with the reference density-functional based pair potential.

III. SIMULATION OF THE GLASSY STATE

A. Production of the glassy state

In the simulation using model I, we utilized the glassy state that was prepared in an earlier study.[7,25] It was produced by quenching the system rapidly from the equilibrium liquid domain to the temperature much below its melting point, which allowed to avoid a possible transformation into an ordered solid phase. The structural stability of this glassy phase had been tested in an extensive MD run investigating its dynamics,[25] whereby no appreciable drift in the potential energy had been observed. In the present study, this model was explored at $\rho=0.84$ and $T=0.2$, in reduced units.[26] This temperature is about 40% of the estimated melting point.[25]

The procedure of preparing the glassy phases using models II and III was started by simulating the liquid state at $T=2300$ K which had been properly equilibrated in a run of 4000 fs. Then the systems were subjected to a rapid quenching which reduced the temperature to $T=100$ K. The quenching was performed in a 3000 fs run, which corresponds to the cooling rate of 7.3×10^{14} K/s. The cooling was done by continuously decreasing the value of the temperature parameter in the Nosé algorithm. The value used for the
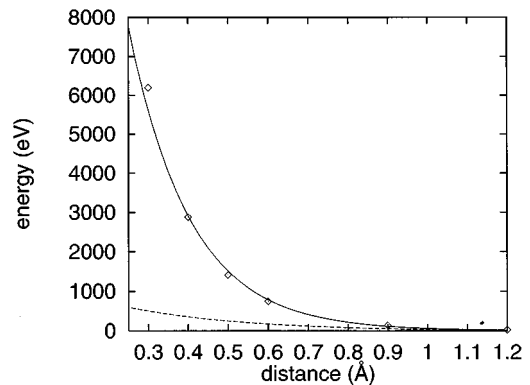

FIG. 1. The energy of Ni-Ni interaction calculated by the modified (solid line) and original (dashed line) EAM models. The high-energy pair potential, obtained from density-functional calculations, is shown by squares.

Nosé thermal inertia parameter was 1.0×10^{-44} Js^2. The glassy models II and III were simulated at the number density 8.8×10^{28} 1/m^3, which is about 4% smaller than the density of fcc solid Ni at zero temperature. This was intended to account for the density reduction caused by the disordered packing in the glass. After having been rapidly cooled, the system was allowed to relax for 30 000 fs, after which its structural characterization was performed. The relaxed system was used as a starting configuration for the radiation damage simulations. We varied the quenching routine by using different cooling rates as well as a different method of cooling that was based on the reduction of the kinetic energy by velocity scaling. These variations in the preparation procedure, however, have not been found to result in any appreciable differences in the structure of thus produced glassy phases. This observation is supported by a recent study by Vollmayr et al.[27] They found that a variation of the cooling rate over four decades leads to a 1–2% change in the enthalpy and other structure-dependent bulk characteristics of the glassy state. The simulations with the models II and III were performed using a routine in which the time step was adjusted so that the displacement of the fastest atom in one step was constrained to 0.02 Å .

B. Structural characterization

An approximate evaluation of ISRO in the glassy states produced can be done using the spherically symmetric pair correlation function $g(r)$ or its Fourier transformation, the structure factor $S(q)$; these are presented in Figs. 2 and 3, respectively. The most prominent feature of the structure factors for all the three simulated models is the pronounced split in the second peak. This peculiarity, characteristic of the metallic glasses, represents an unambiguous evidence that the local order in the simulated structures is dominated by ISRO.

In order to distinguish the structural damage in the glasses induced by irradiation, a detailed quantitative 3D characterization of the local order is indispensable. The basic difficulty in the structural analysis of disordered condensed systems arises from the fact that, in contrast to crystalline structures, there exist no universal analytically describable reference model suitable for their characterization. Therefore, the analysis is usually focused on the statistics of some representative local structural units. In this study, we adopted the method that involves statistical description of different sorts of bonded pairs of atoms. Two particles are regarded as a bonded pair of neighbors if the separating distance does not exceed the specified bond length. The pair is then characterized by the pattern of its common neighbors. If these form a closed bonded ring, the pair is labeled by the number of atoms in the ring. The fivefold pair, a pentagonal bipyramid, is of special interest since it is the basic element of the icosahedral order, as illustrated in Fig. 4. Our analysis also included sixfold and fourfold pairs that are constituent elements of periodic structures. The statistical balance between these and the fivefold pairs thus characterizes the degree of ISRO. Furthermore, we identified the atoms with icosahedral coordination. An atom was regarded as a center of 13-atom icosahedron if it had 12 neighbors and it formed fivefold pairs with all of these.

The described structural analysis was carried out assuming the maximum bond length to be 1.6 r.u. for model I, and
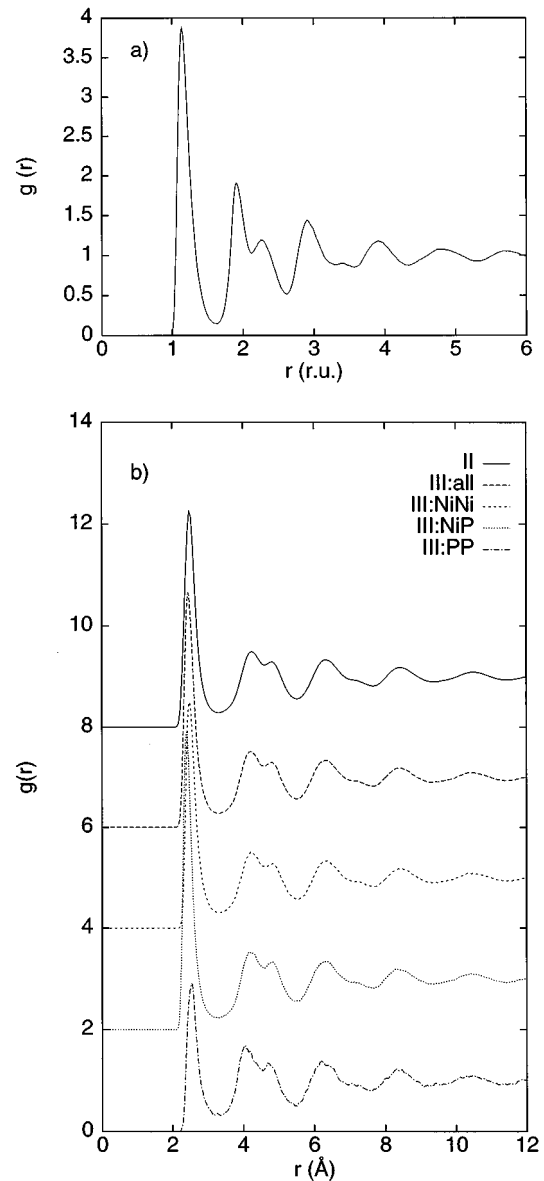

FIG. 2. The pair-correlation functions for the three studied systems: (a) model I and (b) models II and III. In (b) also the partial pair-correlation functions are shown.

3.4 Å for models II and III. The statistics of bonded pairs for the prepared glassy systems is presented in Table III. For comparison, we also give the corresponding statistics for the Lennard-Jones system, where available. The three glassy structures investigated here demonstrate very similar patterns of bond distribution. The local configurations are clearly dominated by the fivefold symmetry, which indicates the presence of a pronounced ISRO. This is indeed confirmed by the large number of icosahedrally coordinated atoms in these models. The presented statistics of local order in the simulated glasses shows a dramatic contrast with the corresponding results for the Lennard-Jones system,[7] where the share of icosahedra is negligibly small. The largest degree of ISRO is observed in model I. In the two-component model III the number of icosahedra is 25% larger than in the one-component model II. Presumably, this indicates the important role of chemical ordering in formation of ISRO.
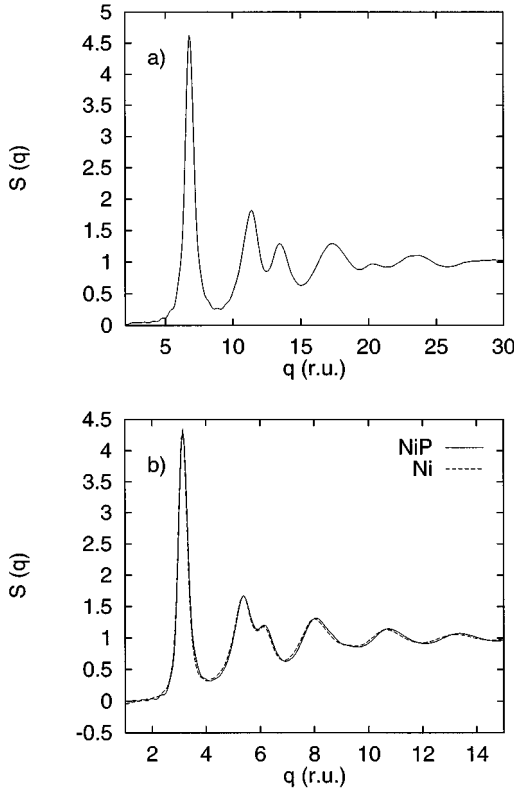
FIG. 3. The structure factors for the three studied systems: (a) model I and (b) models II and III.

FIG. 4. A fivefold bonded pair (emphasized) forming the upper segment of a 13-atom icosahedron.

We have also tested the structural stability of the models II and III. For that purpose, the dynamics of their structural statistics was monitored during 100 ps runs after the 30 ps relaxation. No consistent drift in either the bond distribution or in the icosahedra statistics was found. Therefore, we conclude that the simulated models represent glassy phases which are in a state of metastable equilibrium, at least in the time scale accessible for simulation. This guaranteed a safe platform to perform the radiation damage simulations, because the structural changes due to internal system evolution could be excluded.

IV. RADIATION DAMAGE SIMULATION

The aim of the present radiation damage simulations was to investigate the structural changes caused by the collision cascade following a single collision between a fast moving particle (e.g., a neutron) and an atom. This was simulated assigning an assumed momentum transfer to an atom which is called the primary knock-on atom (PKA). In order to

maximize the allowed extent of the collision cascade, which is limited by the boundaries of the simulation cubic cell, the direction of momentum transfer was chosen [110], in the cell axes notation. Although the [111] direction appears to be the most suitable for the above purpose, [110] was chosen because of its convenience for visualization, which will become apparent below. Correspondingly, PKA was selected as a closest atom to the point with coordinates $x = y = a$ and $z = L/2$, where a is the second nearest-neighbor distance, and L is the size of the simulation box. Because of large velocities involved at the initial stages of the collision cascade, the time step was subject to dynamical adjustment so that the maximum atomic displacement in one integration step did not exceed 0.01 r.u. for model I and 0.02 Å for models II and III. It has to be noted that, in the case of Verlet algorithm employed here, the variable time-step method described leads to variation in the total energy. However, this is not expected to have a significant effect on the evolution of the nonequilibrium state which we examine in this simulation, created by a large-scale local energy release.

This simulation explored the knock-on energies ranging from 100 eV to 10 keV. We present here representative results corresponding to the energy of 5 keV for model I and 4 keV for models II and III. The results have been averaged over five directions of the PKA impact momentum which included [110]. Each of the four other directions is 5 degrees apart from [110]; two of these belong to a plane defined by [110] and [001], and the other two are in the plane perpendicular to the latter one.

In order to perform the simulation in the center-of-mass reference frame, the momentum assigned to PKA, divided by the number of atoms in the system, was subtracted from each constituent atom. Scaling up the velocity of PKA also increases total kinetic energy of the system. In a macroscopic system the inserted energy would produce a sharp thermal spike at the vicinity of PKA and then dissipate into the surrounding structure causing negligible variation of its temperature. This simulation uses keV range of the PKA energies which results in a considerable increase in the total temperature, even for the system size we employed. The total temperature shift would change considerably the statistical characteristics of the simulated structure, thus inducing uncertainty in the analysis of its evolution caused by the initial collision, and therefore should be avoided. In the earlier ra-

TABLE III. Statistics of the bonded pairs and icosahedra in the prepared glassy phases, compared with those for the LJ system.

Model	Fourfold	Fivefold	Sixfold	Icosahedra
I	4450	60450	12250	1750
LJ		17552		33
II	11400	45500	19300	445
III	10950	46300	18900	555

diation damage simulation,[5] a region at the simulation box boundaries was assumed where the velocity of an entering atom was scaled down, imitating thermal coupling of the system to the surrounding heat reservoir. This routine tends to reflect the heat pulse back, and to minimize this effect the scaling region should be made as large as possible. However, the inevitable disadvantage of a large scaling region is the reduction in the size of the available free part of the system. In the present study a different approach was adopted based on the Nosé algorithm. This algorithm can be viewed as adding a friction term to the equations of motion, which is assumed to describe the coupling to the surrounding heat bath. The good thermal conductivity observed in metals mediated by the electrons requires tight coupling in the above algorithm resulting in a rapid energy outflow from the computational cell. However, the use of this algorithm in the initial nonequilibrium stages of the collision cascade leads to too strong a damping of the velocities of the fastest atoms due to the global friction coefficient. Therefore in the present study the Nosé algorithm was turned on only when the maximum particle velocity observed in the system had decreased below the value of five times the average particle velocity.

We adopted the approach proposed by Laakkonen and Nieminen[5] who analyzed the structural changes in the irradiated system by monitoring the statistics of two types of defects, interstitials, and vacancies. The former were associated with atoms experiencing (negative) local pressure considerably beyond the average value. The value of pressure limit used in interstitial analysis was -6.0 r.u. for model I and correspondingly -1.92×10^{10} Pa for models II and III. A vacancy was defined as a sphere that that could be inserted in a structural void without touching the adjacent atoms. Its radius was assumed to be 1.1 r.u. for model I and the corresponding value for models was II and III was 2.0 Å. The bond analysis and the interstitial statistics were calculated every 50 time steps, while the computationally costly counting of vacancies was done with the interval of 200 time steps. The chosen criteria for the interstitials and vacancies guaranteed that a nonzero number of both defects existed already in the unperturbed configuration, making thus the possible permanent changes in these quantities caused by the collision cascade easier to detect.

V. RESULTS AND DISCUSSION

Figures 5–7 present the dynamics of the quantities describing the local order. The figures give a comprehensive picture of the structural evolution that follows the simulated event of primary collision. The quantities monitored in the simulation runs were the statistics of local structural units obtained in the bond analysis as described above. Besides these, we also analyzed the variation of the number of interstitials and local voids (vacancies); the latter was found to be an important characteristics of the structural evolution of the glassy systems explored in this study. In all the figures, the time zero corresponds to the instant of the PKA recoil event.

There appears to be good agreement between the respective curves describing the evolution of the bond statistics for all the three models studied. The local energy release caused by the primary collision is expected to transform the equilibrium glassy configuration characterized by predominantly
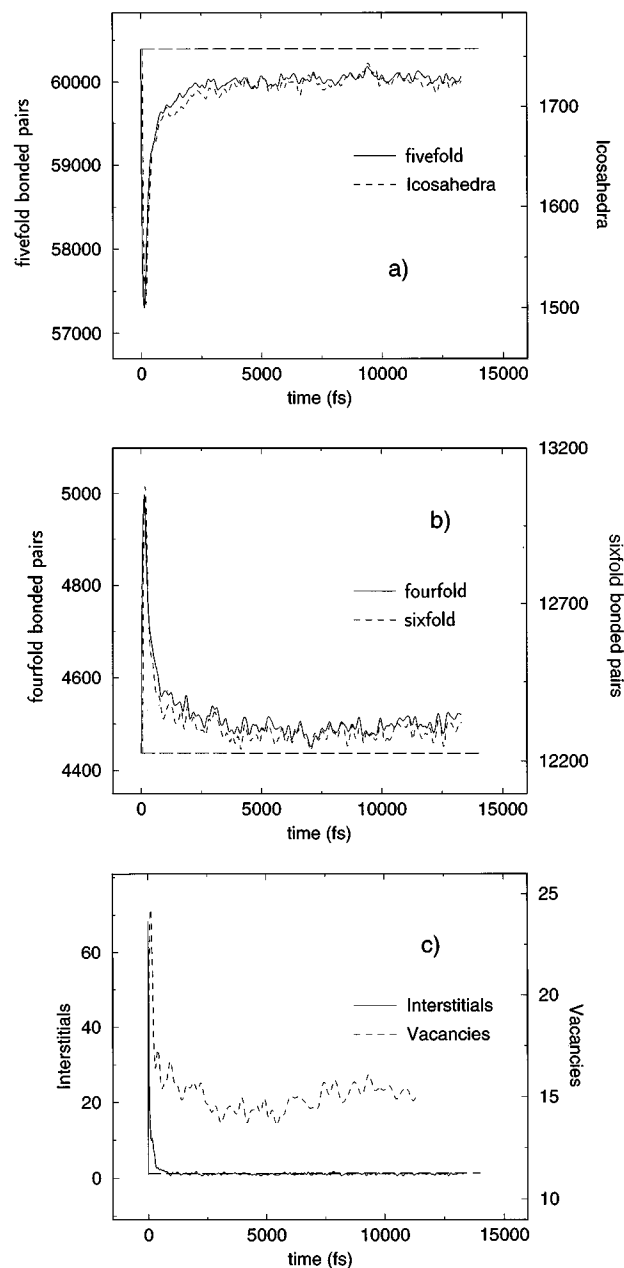

FIG. 5. The structural evolution after a 5 keV knock-on in model I: the number of (a) fivefold bonded pairs and icosahedra, (b) four- and sixfold bonded pairs, (c) vacancies and interstitials. The horizontal dashed line in each plot represents the averaged value of the corresponding quantity in the unperturbed system.

tetrahedral packing, into a less energetically favorable structure. The number of fivefold bonds, indeed, demonstrates an initial drop, followed by a steady and slow increase. The number of icosahedra, as expected, repeats this behavior. Simultaneously, the observed reduction in the degree of the local fivefold symmetry results in the correspondent sharp transient increase in the number of sixfold and fourfold bonds. The latter, representing nontetrahedral local structural units, are especially significant since variation in their statistics produces a major contribution to the increase in the potential energy caused by the radiation-induced structural transformation.
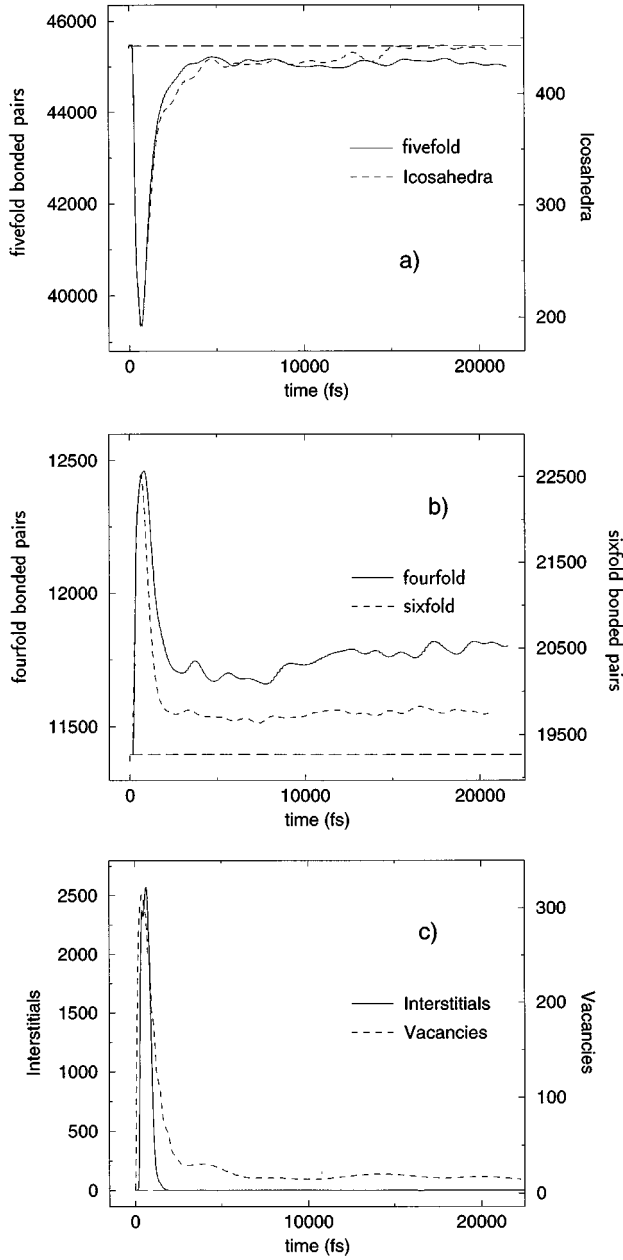
FIG. 6. The structural evolution after a 4 keV knock-on in model II: the number of (a) fivefold bonded pairs and icosahedra, (b) four- and sixfold bonded pairs, (c) vacancies and interstitials. The horizontal dashed line in each plot represents the averaged value of the corresponding quantity in the unperturbed system.
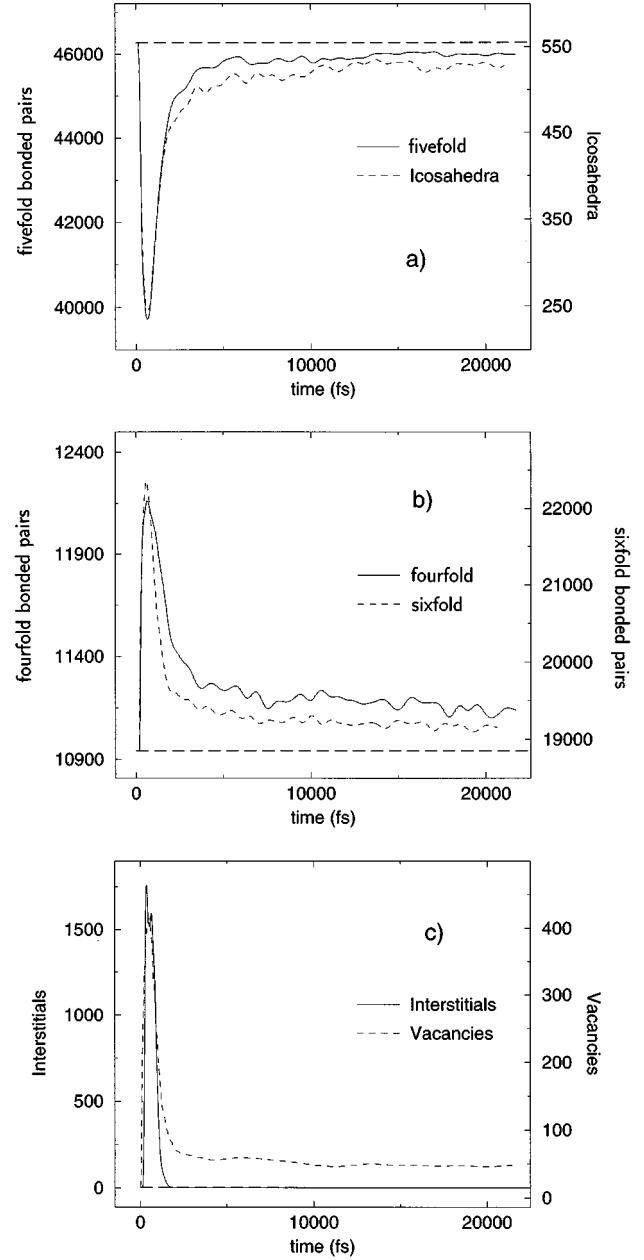
FIG. 7. The structural evolution after a 4 keV knock-on in model III: the number of (a) fivefold bonded pairs and icosahedra, (b) four- and sixfold bonded pairs, (c) vacancies and interstitials. The horizontal dashed line in each plot represents the averaged value of the corresponding quantity in the unperturbed system.

A major result of this study which can be seen from the presented results of structural analysis is that the perturbation of the equilibrium configuration induced by the local energy release eventually results in an appreciable degree of permanent structural damage. The quantities representing the statistics of local units, although recovering partly after the initial sharp variation, do not return to the level observed in the unperturbed structure. The model II, however, represents an exception in that respect: its number of icosahedra returns to the corresponding value of the unperturbed configuration. Nevertheless, even in this case, there is a net decrease in the number of fivefold bonds as compared with the correspond-

ing unperturbed level. In addition, in model II the number of fourfold bonds indicated a slow, continuous increase during the recovery period. This feature could not be observed in model III and this observation can presumably be attributed to the two-component nature of model III and the stabilizing effects due to the added phosphorus atoms.

The dynamics of the spatial distribution of icosahedra in the process of radiation-induced structural transformation in model I is visualized in Fig. 8. The three plots presented depict instantaneous configurations of the atoms possessing icosahedrally ordered first-neighbor shell as projected on the xy plane. Filled circles correspond to the icosahedra confined
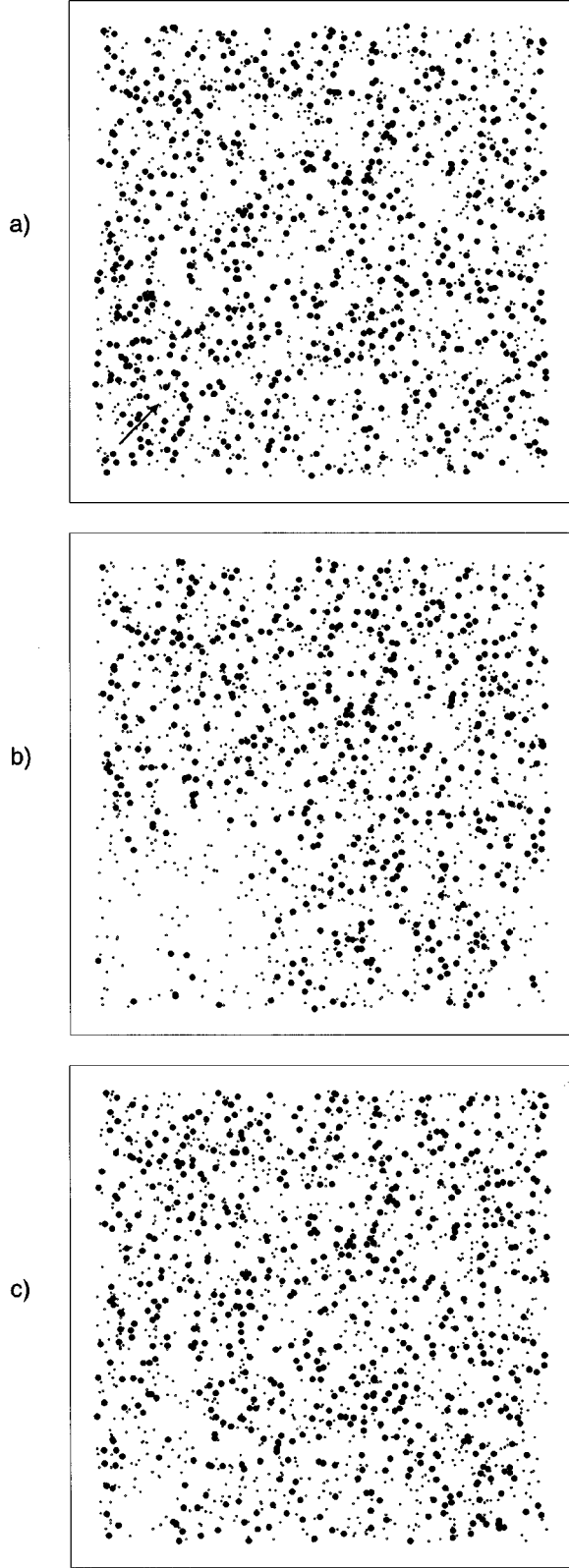
FIG. 8. The centers of icosahedra as projected on the xy plane; those confined in the layer $0.3L < z < 0.7L$, L being the size of the main simulation cube, are marked by filled circles, the rest are shown by dots. (a) unperturbed configuration at the moment of collision; (b) and (c) represent the configurations 360 fs and 4300 fs after the primary collision moment, respectively. The arrow originates from the PKA position and indicates the knock-on direction.

within a layer which is defined as $0.3L < z < 0.7L$, L being the size of the main simulation cube; the rest of the icosahedra are shown by dots. The arrow indicates the direction of the primary collision, with its origin located at the PKA. Figure 8(a) represents unperturbed configuration as it was at the moment of the primary collision. The configuration depicted in Fig. 8(b) corresponds to the time instant 360 fs after the collision when the number of icosahedra is passing through its minimum (compare with Fig. 5). The reduction of icosahedral order in the region affected by the collision cascade is apparent. Finally, Fig. 8(c) shows the spatial distribution of icosahedra after a 4300 fs relaxation run following the primary collision. This time interval appears to be sufficient for considerable restoration of the icosahedral order in the area where the structure has been damaged by the simulated irradiation. It is clear, however, that the recovery is not complete.

The described transformation of ISRO in the simulated models caused by the local collision cascade cannot be immediately compared with the respective structural evolution of the LJ glassy model investigated by Laakkonen and Nieminen[5] because of the qualitative difference in the local order of the two systems. But we can compare the respective variations in the statistics of other structural defects induced by irradiation, interstitials, and vacancies. The number of interstitials, after the sharp transient increase, fully recovers its unperturbed value in all the models studied. Therefore, interstitials do not contribute to the residual structural damage that we observed in the irradiated systems after their relaxation. In that respect, the observed behavior agrees well with that observed in the LJ glass. However, as far as the vacancies are concerned, the systems investigated here demonstrate a striking distinction in their structural evolution. In contrast to the LJ case, the number of vacancies does not return to its initial level. Thus the glassy structures with pronounced ISRO appear to be able to sustain, even after the equilibration, a considerable degree of these defects that have been produced by the collision cascade.

VI. CONCLUSIONS

In the MD study presented here, we have investigated the structural evolution of metallic glasses subjected to irradiation. We focus on the analysis of the radiation-induced transformation in ISRO, a distinctive structural feature of metallic glasses which is possessed by all the three models explored here. For that purpose, we employ the bond analysis method which, together with the vacancy analysis method, has been proved to be a powerful tool of the structural investigation. Using this approach, we obtain a detailed picture of the evolution of the local order during the equilibration period following the initial collision event. The simulated glassy structures have demonstrated a considerable degree of residual structural damage, reducing the initial degree of ISRO, which however survives even after irradiation.

A most interesting finding of this simulation is that all the three models investigated show a considerable increase in the number of vacancies. This observation is in sharp contrast with the earlier simulation of the radiation damage in the Lennard-Jones glass.[5] It appears that the systems with pronounced ISRO possess a generic ability to sustain a con-

siderable density of vacancies while remaining in the equilibrium state. This conclusion is consistent with the observation[9] that the model I, having been explored in the equilibrium liquid domain, demonstrates a large rate of vacancy-related hopping diffusion. The presence of vacancies is also apparent in the structure of the quasicrystal that this system was found to form.[10] This remarkable distinction of the systems with ISRO can be attributed to the singular stability of the local icosahedral configurations as compared with the corresponding structural units characteristic of other kinds of short-range order. In the macroscopic scale, the local increase in the number of vacancies is expected to dissipate in the bulk of the glassy structure due to the usual vacancy-diffusion mechanism. However, if a glassy sample is subjected to an intensive flux of high-energy particles during a sufficiently long time period, the increase in the total density of vacancies might be considerable, resulting in the change of the volume. This conjecture seems to be consistent with the experimental observations.[28]

*Electronic address: Tomi.Mattila@hut.fi

†Electronic address: Risto.Nieminen@hut.fi

‡Electronic address: mik@pdc.kth.se

[1] F. C. Frank, Proc. R. Soc. London Ser. A **215**, 43 (1952).

[2] D. Schechtman, L. Blech, D. Gratias, and J. W. Cahn, Phys. Rev. Lett. **53**, 1951 (1984).

[3] S. Sachdev and D. Nelson, Phys. Rev. B **32**, 1480 (1985).

[4] J.-O. Nilsson, A. Hultin Stigenberg, and P. Liu, Metall. Mater. Trans. A **25A**, 2225 (1994).

[5] J. Laakkonen and R. M. Nieminen, Phys. Rev. B **41**, 3978 (1990).

[6] M. Dzugutov, J. Non-Cryst. Solids **156-158**, 173 (1993).

[7] M. Dzugutov, Phys. Rev. A **46**, R2984 (1992).

[8] S. Nosé, Mol. Phys. **52**, 255 (1984).

[9] M. Dzugutov, Europhys. Lett. **26**, 533 (1994).

[10] M. Dzugutov, Phys. Rev. Lett. **70**, 2924 (1993).

[11] D. Holland-Moritz, D. M. Herlach, and K. Urban, Phys. Rev. Lett. **71**, 1196 (1993).

[12] S. R. Elliott, J. Phys. Condens. Matter **4**, 7661 (1992).

[13] S. R. Elliot, *Physics of Amorphous Materials* (Longman, New York, 1983).

[14] M. S. Daw and M. I. Baskes, Phys. Rev. B **33**, 7983 (1986).

[15] Ch. Hausleitner and J. Hafner, Phys. Rev. B **45**, 115 (1992).

[16] Ch. Hausleitner and J. Hafner, Phys. Rev. B **45**, 128 (1992).

[17] For the details of the EAM parametrization the reader is asked to contact the authors at Helsinki University of Technology.

[18] R. A. Johnson, Phys. Rev. B **37**, 3924 (1988).

[19] J. H. Rose, J. R. Smith, F. Guinea, and J. Ferrante, Phys. Rev. B **29**, 2963 (1984).

[20] D. J. Oh and R. A. Johnson, J. Mater. Res. **3**, 471 (1988).

[21] C. Kittel, *Introduction to Solid State Physics*, 5th ed. (Wiley, New York, 1976).

[22] Calculations performed by T. Korhonen, Laboratory of Physics, Helsinki University of Technology, Finland.

[23] J. Keinonen, A. Kuronen, P. Tikkanen, H. G. Börner, J. Jolie, S. Ulbig, E. G. Kessler, R. M. Nieminen, M. J. Puska, and A. P. Seitsonen, Phys. Rev. Lett. **67**, 3692 (1991).

[24] Calculations performed by A. P. Seitsonen, Laboratory of Physics, Helsinki University of Technology, Finland.

[25] M. Dzugutov, Mater. Sci. Eng. A, **134**, 921 (1991).

[26] The calculated quantities for model I are expressed in the Lennard-Jones reduced units (r.u.) which were used in the definition of the pair potential Ref. (7). The models II and III were simulated using SI units.

[27] K. Vollmayr, W. Kob, and K. Binder (unpublished).

[28] P. Garoche, Y. Calvayrack, W. Cheng, and J. J. Veyssie, J. Phys. F **12**, 2783 (1982).